

VISION-LANGUAGE MODELS UNLOCK TASK-CENTRIC LATENT ACTIONS

000
001
002
003
004
005
006
007
008
009
010
011
012
013
014
015
016
017
018
019
020
021
022
023
024
025
026
027
028
029
030
031
032
033
034
035
036
037
038
039
040
041
042
043
044
045
046
047
048
049
050
051
052
053
Anonymous authors
Paper under double-blind review

ABSTRACT

Latent Action Models (LAMs) have rapidly gained traction as an important component in the pre-training pipelines of leading Vision-Language-Action models. However, they fail when observations contain action-correlated distractors, often encoding noise instead of meaningful latent actions. Humans, on the other hand, can effortlessly distinguish task-relevant motions from irrelevant details in any video given only a brief task description. In this work, we propose to utilize the common-sense reasoning abilities of Vision-Language Models (VLMs) to provide promptable representations, effectively separating controllable changes from the noise in unsupervised way. We use these representations as targets during LAM training and benchmark a wide variety of popular VLMs, revealing substantial variation in the quality of promptable representations as well as their robustness to different prompts and hyperparameters. Interestingly, we find that more recent VLMs may perform worse than older ones. Finally, we show that simply asking VLMs to ignore distractors can substantially improve latent action quality, yielding up to a six-fold increase in downstream success rates on Distracting MetaWorld.

1 INTRODUCTION

Latent action models [42, 53] have quickly become integral to the pre-training pipelines of leading Vision–Language–Action (VLA) systems [5, 7, 58, 6, 25]. By inferring compact, semantically meaningful latent action representations at scale, Latent Action Models (LAM) mitigate the scarcity of high-quality action-labeled data, giving a promise to unlock vast amounts of unlabeled videos [33]. Removing the data bottleneck facilitates further scaling in embodied AI and robotics; consequently, any improvements to LAMs can have outsized downstream impacts.

Unfortunately, most LAMs [42, 53, 10, 18] to date have been trained on relatively clean datasets, where changes between observations can be explained almost entirely by ground-truth actions—such as in static scenes with a single manipulator. In contrast, real-world data often contains numerous action-correlated distractors, including background human movement or other spurious correlations. As shown by Nikulin et al. [36], Zhang et al. [56], without explicit supervision, LAMs struggle to disentangle controllable changes from noise, completely failing to produce meaningful latent actions in the presence of action-correlated distractors. While providing supervision via true actions can be effective [36], it is not scalable — especially in domains where these actions are impossible to obtain, such as egocentric human videos.

Humans, however, interpret the world through semantics rather than raw pixels, and with only a brief task description can easily separate task-relevant features from irrelevant details in any video. Wouldn’t it also be convenient to simply ask LAM to focus on the relevant features, e.g. robotic arm, and ignore any other details? Inspired by the work of Chen et al. [9], Huang et al. [24] on promptable representations, we propose to utilize the common-sense reasoning abilities of modern Vision-Language Models (VLMs) as an unsupervised approach for effectively separating controllable changes from noise, thereby restoring the LAM’s ability to recover ground-truth actions even in the presence of distractors.

In this work, we present our investigation on whether promptable representations produced by prompting VLMs to focus on task-specific details can serve as an effective target for latent action learning in the presence of distractors. Using Distracting MetaWorld as our main environment (Section 3), we begin from a simple demonstration experiment, showing that limitations of LAM

054 can be mitigated with the right target (Section 4). We then conduct large-scale benchmarking
 055 of different VLMs, comprising over 29k+ experiments, to assess their effectiveness at providing
 056 promptable representations (Section 5), revealing substantial variation in quality and robustness to
 057 hyperparameters. Finally, using the best setup found, we demonstrate that without any supervision
 058 **with true actions**, promptable representations can significantly improve latent action quality and
 059 downstream performance, increasing the success rate six-fold (Section 6).

060 2 BACKGROUND

063 **Problem setting.** We consider a setting of offline imitation learning from observation [32, 46],
 064 which closely matches the regime increasingly utilized by the field of embodied AI [33, 7, 5]
 065 (e.g. robotics). Our goal is to pre-train a policy $\pi(o|a)$, given a large dataset of expert trajectories
 066 $\mathcal{D} := \{(o_i^n)\}_{i=1}^{\tau}$, containing observations but not actions (e.g. videos), and a limited number of real
 067 action labels. Ideally, the pre-trained agent should achieve maximum performance (e.g. success rate)
 068 in the environment after fine-tuning with a minimum amount of action-labeled data. The commonly
 069 considered ratio of labeled to unlabeled data is around 2 – 10% in the existing work [57, 36], while
 070 in our experiments, we consider a ratio as low as < 1%.

071 **Promptable representations.** A VLM processes multimodal inputs by encoding both the image
 072 and text before generating an output. The resulting sequence of token embeddings has length I
 073 + P + O , where I represents the visual token count, P represents the prompt token count, and O
 074 corresponds to the number of tokens produced during generation. We follow the Chen et al. [9] and
 075 define promptable representations simply as a process of obtaining observation embeddings from
 076 the VLMs given a task-specific prompt and some extraction and aggregation strategy. We obtain
 077 such representations from the last and next-to-last layers [9]. In contrast to the Chen et al. [9], Huang
 078 et al. [24] we cannot learn pooling from the data to better predict true actions or obtain better reward.
 079 Thus, we experiment only with simple fixed strategies, such as taking the mean over all embeddings
 080 or taking only the embedding of the last token from either prompt or the generated answer. **Thus, the**
 081 **final promptable representations is always just a single vector $s \in \mathbb{R}^D$, where D is a VLMs hidden**
 082 **size.**

083 **Latent action models.** Given the dataset of observations $\mathcal{D} := \{(o_i^n)\}_{i=1}^{\tau}$, latent action models
 084 (LAM) [41, 17, 42] try to infer latent actions z_t such that they are maximally predictive of observed
 085 transitions (o_t, o_{t+1}) while being minimal [42], i.e. describe changes only relevant to control. After
 086 pre-training, LAM is used to supply latent actions for **behavioral cloning (BC)** on unlabeled dataset
 087 to obtain useful behavioral priors. As a final stage, small decoder is trained to map from latent to
 088 ground-truth actions on a small number of labels.

089 Modern LAMs [6, 53, 12, 11, 10, 18] mostly follow the same high-level architecture introduced by
 090 LAPO [42], which uses a combination of inverse (IDM) and forward (FDM) dynamics models to
 091 infer latent actions. Given a transition (o_t, o_{t+1}) , IDM first infers latent action $z_t \sim f_{\text{IDM}}(\cdot | o_t, o_{t+1})$,
 092 which FDM further uses to predict the next observation $\hat{o}_{t+1} \sim f_{\text{FDM}}(\cdot | o_t, z_t)$. Both models are
 093 trained jointly to minimize the loss $\mathcal{L}_{\text{MSE}} = \mathbb{E}_{(o_t, o_{t+1}) \sim \mathcal{D}} \left[\| f_{\text{FDM}}(f_{\text{IDM}}(o_t, o_{t+1}), o_t) - o_{t+1} \|^2 \right]$.

094 **Limitations of latent action models.** Recent studies highlighted LAM failure when action-correlated
 095 distractors are present [36, 28, 56]. While they can recover ground-truth actions when only control-
 096 lable changes are present, real-world videos typically involve both controllable factors and exogenous
 097 noise (e.g., people moving in the background). In such cases, LAMs cannot disentangle the dynamics,
 098 leading latent actions to primarily capture noise, which makes them useless for imitation learning.
 099 Both Nikulin et al. [36], Zhang et al. [56] proposed providing supervision with a small number of true
 100 actions during LAM training to help identify controllable changes. While this solution is effective, it
 101 is not generalizable, as in many domains, such as egocentric human videos [52], it is not possible to
 102 obtain true actions in a reasonable way.

103 3 EXPERIMENTAL SETUP

104 **Environments and datasets.** In contrast to Nikulin et al. [36], we use MetaWorld Multi-Task 10
 105 [54] as our primary benchmark, as it provides greater realism than Distracting Control [44], while
 106 being lightweight enough to allow experimentation with VLMs under limited resources. We modify

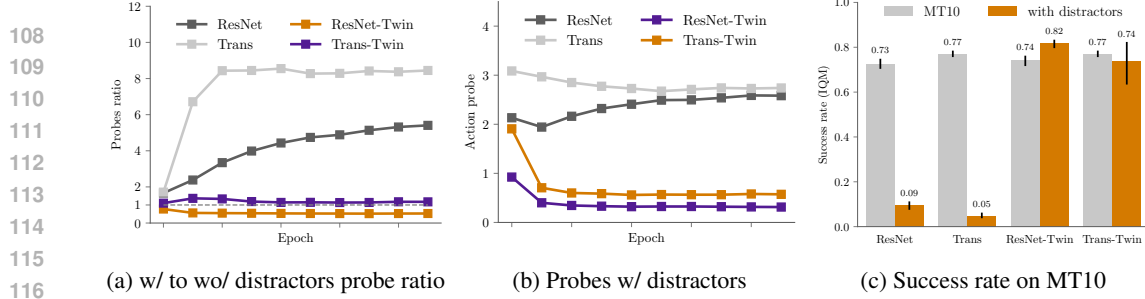


Figure 2: Demonstration that quality of latent actions learned by LAPO completely degrades in the presence of distractors, which results in almost zero success rate. **Action probe represents MSE of a linear probe trained to predict real actions from latent actions. See Section 3 for detailed explanation.** We show that with the ideal target for FDM, which perfectly disentangles controllable features from the noise, performance may be restored, serving as a main motivation for us to explore promptable representations. We use three random seeds and report IQM and 95%-CI based on stratified bootstrapping, following the Agarwal et al. [1]. See Section 4 for details.

MetaWorld to include distracting dynamics videos in the background, using the same DAVIS videos as in Nikulin et al. [36]. We also move the default camera position farther back and remove borders around the table to include more of the background video in the observation, making latent action learning more challenging. See Figure 1 for a visualization.

We follow the standard three-stage pipeline [42, 53, 36]: (1) pre-train the LAM, (2) train **behavioral cloning (BC)** agent on latent actions, and (3) train a decoder head on a small number of true-action labels. For each task, we collect 5k trajectories from the scripted experts provided by MetaWorld and up to 16 additional labeled trajectories for the final stage, which is less than 1% of the full datasets.

Evaluation. For evaluation, we follow standard metrics similar to Nikulin et al. [36]: **action probe** and **success rate**. Specifically, we train linear probes to predict real actions from the latent ones during LAM training, while stopping the gradient through the latent actions. The final MSE serves as our quality metric, as it indicates whether the latent actions encode the real ones. This metric is also used for hyperparameter tuning, which may be impractical in real-world settings but allows us to estimate the upper-bound performance of each method for fair comparison.

However, as Nikulin et al. [36] notes, linear probing has a key limitation: it can reveal whether true actions are present in the latent space, but it does not guarantee minimality, meaning that exogenous noise may still be encoded. To preserve this guarantee, we fix the latent action dimensionality to 128 for all methods, which at least allows us to rank quality under equal information bottleneck. Finally, to measure the true usefulness of latent actions, we evaluate the success rate in the environments after fine-tuning on true action labels.

Latent action model architecture. We use the architecture proposed by Schmidt & Jiang [42], omitting action quantization, due to its harmful effect [36, 31, 51]. We use frame stacking, but only in IDM, while FDM uses only the current frame to predict the next, as in Chen et al. [10]. Other than that, in our main experiments, we do not use any improvements upon LAPO (if not explicitly stated otherwise), such as augmentations or multi-step predictions in FDM [36, 10, 53, 12], to remove possible confounders on latent action quality. When predicting in the latent space instead of images, we follow Nikulin et al. [36] and use multiple MLP blocks similar to those used in Transformers [47]. For action decoder head, we use a small three-layer MLP. See Section C for hyperparameters used.



Figure 1: Visualization of observations with and without distractors in our modification of MetaWorld environment.

4 THE IMPORTANCE OF RIGHT TARGET

We begin with a demonstration experiment to show that the limitation of LAMs in the presence of distractors arises entirely from the poor target used in the forward dynamics model (FDM), rather than from any flaw in the overall idea or architecture. By LAM construction, latent actions are optimized

162 to maximally explain the dynamics. Therefore, the root of the failure to recover true actions lies in
 163 the dynamics we predict, which is directly determined by the target in FDM: $\hat{o}_{t+1} \sim f_{\text{FDM}}(\cdot | o_t, z_t)$.
 164 What would be the ideal target for FDM? And if it exists, what would be the final performance?
 165 Could LAM recover the ground-truth actions despite distractors in the input observations to IDM and
 166 FDM? If not, the idea with promptable representations would be impractical.

167 **Setup.** To answer these questions we construct a special dataset with twin observations for each task:
 168 during data collection we render and save same observation with and without distractors. Next, during
 169 training we feed observations with distractors as inputs to IDM and FDM, but as the target for FDM
 170 we use next observation without distractors. As the actual controllable changes are preserved (the
 171 underlying state is the true next state), it serves as a target with ideal disentanglement of controllable
 172 features from exogenous noise (see Figure 1). To show that existing limitations are agnostic to the
 173 architecture of FDM and IDM, we explore both ResNet [42] and spatio-temporal transformer [6, 53]
 174 backbones.

175 **Results.** First of all, as can be seen in Figure 3, we confirm
 176 that in our domain simply adding distractors results in complete
 177 degradation of latent actions quality regardless of backbone
 178 used. This subsequently leads to almost zero success rate after
 179 fine-tuning on true actions (see Figure 2c), which does not
 180 happen without distractors. Ideally, probes should be close to
 181 each other, as real underlying actions are identical between both
 182 settings.

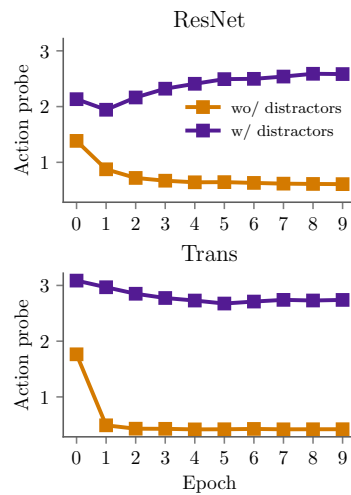
183 Next, in Figures 2a and 2b we show the effect of using perfect
 184 targets during LAPO training (with -Twin postfix). To better
 185 illustrate the trend, in Figure 2a we report the ratio of probes
 186 with and without distractors for each method. With the ideal
 187 target probes immediately drop to the level of LAPO without
 188 distractors, and ratio converges to one. To our surprise, it is in
 189 fact possible to get even better result, as LAPO-ResNet achieves
 190 ratio below one, i.e. outperforming LAPO-ResNet without
 191 distractors. We attribute this to the implicit augmentation effect
 192 of distractors. Finally, improvement in latent action quality
 193 directly results in leveling success rates (see Figure 2c).

194 Overall, this result supports that the right target is the key
 195 to unlock latent action learning in the presence of distractors.
 196 Although these experiments may seem obvious in hindsight,
 197 they allow us to convey a key empirical observation about
 198 latent action learning, one that provides the same intuition that
 199 originally led us to explore promptable representations.

201 5 THE PROMISE OF PROMPTABLE REPRESENTATIONS

203 Our main hypothesis is that VLMs, due to their common-sense reasoning abilities, can serve as an
 204 effective unsupervised way of obtaining clean observation representations, which would disentangle
 205 controllable features from the noise. As we demonstrated in the previous section, it would be enough
 206 to unlock latent action learning in the presence of distractors.

207 We have no doubt that most modern VLMs would easily identify the robotic arm location in the
 208 image (like Figure 1) and describe it in detail, even in the presence of background noise. However,
 209 the ability to generate valid text does not necessarily imply that the underlying embeddings are
 210 suitable for our purposes. For a representation to serve as an effective target for LAM, it should
 211 (1) contain task-centric visual information, (2) be minimal by filtering out visual details irrelevant
 212 to the prompt, and (3) remain consistent across dynamics to mimic changes caused by real actions.
 213 Unfortunately, current VLMs are known to struggle with visual focus [40, 43] and pixel-level
 214 understanding [19, 13, 30]. Given these limitations, we begin by benchmarking a wide variety of
 215 modern VLMs to assess their viability, conducting $\sim 29k$ experiments in total. [As an additional
 baseline, we included representations from self-supervised methods such as CLIP \[39\] and DINOv2](#)



200 Figure 3: Baseline LAPO action probes on MT10. Averaged over 3
 201 random seeds. [Action probe represents MSE of a linear probe trained
 202 to predict real actions from latent
 203 actions. See Section 3 for detailed
 204 explanation.](#)

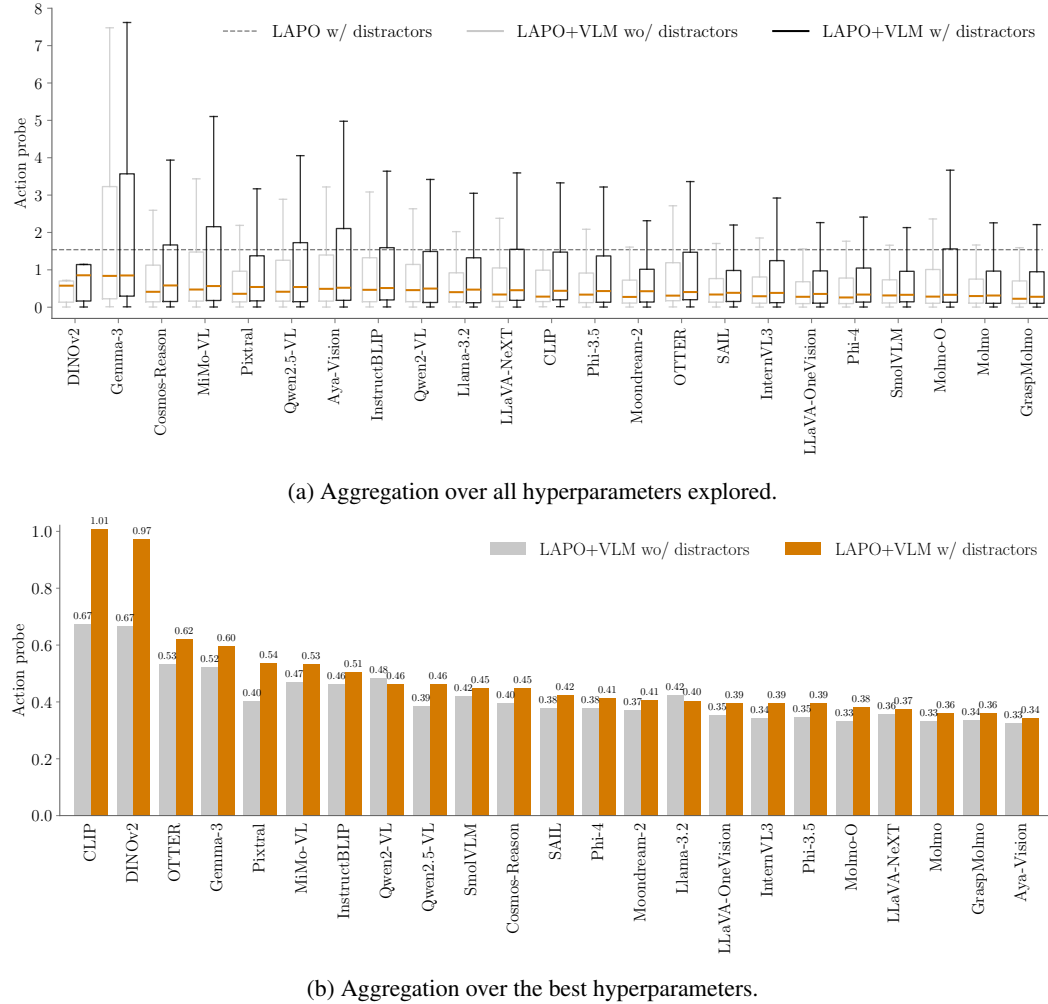


Figure 4: Benchmarking the effectiveness of promptable representations provided by different VLMs for latent action learning on all tasks from MT10. **Action probe** represents MSE of a linear probe trained to predict real actions from latent actions. See Section 3 for detailed explanation. Results aggregated over $\sim 29k$ experiments. Overall, all VLMs provide some improvement over LAPO, with Molmo performing the best and Gemma-3 the worst. For details and exact experimental protocol see Section 5. We additionally provide the ranking for each combination of hyperparameters in the Figure 5.

[37], which are not promptable VLMs but were pre-trained on large amounts of visual data. Based on this benchmark, we then select the most effective VLM along with the best hyperparameters (e.g., prompt, aggregation strategy, and others).

Proper way to evaluate VLMs via small scale experiments. Conducting large scale VLMs evaluation on the full datasets would be prohibitively expensive. Chen et al. [9] proposed assessing prompts via linear probing on small datasets, for example by asking whether task-relevant entities are present in the image and measuring probe accuracy. While feasible, this approach is suboptimal in our setting. Probing representations to predict real actions may help rank prompts for a single VLM, but it cannot reliably compare across multiple VLMs or hyperparameters, since probing does not capture the minimality of representations, an essential property for LAMs. Instead, we directly train LAPO+VLM on a small subset of trajectories, e.g. 64 instead of full 5k, and measure the resulting latent action quality. We validated that hyperparameter rankings obtained in this way transfer reasonably well to the full dataset, although probes can have different values.

Benchmarking general VLMs. We summarize our main benchmarking results in Figure 4 and provide full per-hyperparameter rankings in Figure 5. For each VLM, we evaluated eight prompt variants designed in different styles to exploit diverse VLM capabilities (e.g., CLIP-style captions, pointing,

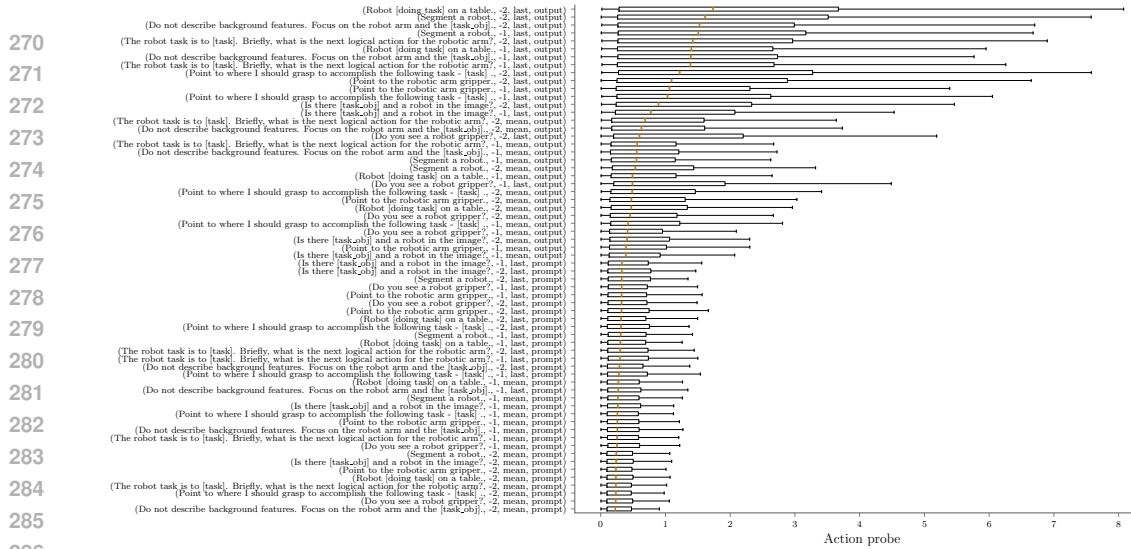


Figure 5: Action probe rankings across all explored hyperparameter combinations. Smaller probe is better. Hyperparameters in order: prompt, layer, reduction type and source of the embeddings. Reported values are averaged over all VLMs, tasks, and settings (with and without distractors). Feel free to zoom in!

segmentation; see Table 1 in Section B). We further varied the source of representations (last vs. next-to-last layer, prompt vs. generated embeddings) and the aggregation strategy (averaging vs. last non-padding token). This yields 64 runs per VLM, per task, per dataset, amounting to roughly 29k experiments in total (including VLMs which we will explore later). The full list of VLMs, including exact model names, sizes, and prompt templates, is provided in Section B.

As can be seen in Figure 4a, overall all VLMs provide some degree of improvement over LAPO in terms of the median action probe. However, some of them, especially Molmo [16], are generally preferable and have lower variance, indicating higher robustness to different hyperparameters. In Figure 4b we visualize ranking by [averaging](#) best scores for each task. While this changes ranking a bit, we still observe that Gemma-3 [45] is the worst and Molmo [16] is consistently the best. Based on Figure 5, we observe that in general, promptable representations aggregated by averaging next-to-last layer prompt embeddings perform the best. From a practical standpoint, this is beneficial, as it eliminates the additional time spent on answer generation. Ironically, the best prompt is *Do not describe background features. Focus on the robot arm and the [task,obj]*, which explicitly asks VLM to filter out distractors.

This brings us to a striking conclusion that state-of-the-art VLMs do not necessarily provide better promptable representations. For example, InstructBLIP [14] outperforms both Gemma-3 [45] and Pixtral [2], despite being considerably older. Furthermore, Cosmos-Reason [4] results indicate that explicit fine-tuning on robotics data is not sufficient to guarantee improved representations. We believe that our results, besides relevance to LAMs, reveal a large blind spot in how VLMs are currently evaluated, with critical implications for robotics and VLA models.

On the other hand, the results from DINOv2 and CLIP (see Figure 4) highlight the vital importance of language conditioning. Although DINOv2 and CLIP may possess helpful inductive biases, for example by attending to moving objects, without language conditioning there is no guarantee that these objects are the ones that are controllable. Both methods achieve the worst latent action quality among all approaches we considered. For instance, OTTER uses the same CLIP model but applies simple training-free filtering using text CLIP embeddings. This small modification significantly improves latent action quality, although still not to the level of native VLMs such as Molmo.

Benchmarking embedding VLMs. In our main benchmark (see Figure 4), we evaluated conventional VLMs, which were not explicitly trained to produce strong unified representations and therefore required heuristics such as embedding averaging. Recently, a new class of embedding VLMs has emerged [27, 34]. These models are designed specifically to learn high-quality, promptable, and multimodal embeddings for zero-shot retrieval. Given the similarity of their objective to ours, one might expect them to perform better. To test this, we evaluated three recent state-of-the-art models

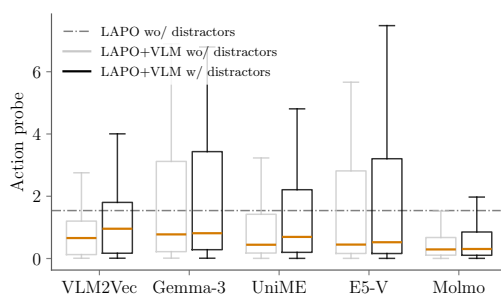


Figure 6: Benchmarking the effectiveness of promptable representations provided by recent *embedding* VLMs for latent action learning on all tasks from MT10. Overall, embedding VLMs, despite their promise, do not deliver any substantial gains compared to traditional VLMs, such as Molmo. We include Gemma-3 and Molmo results here for convinience.

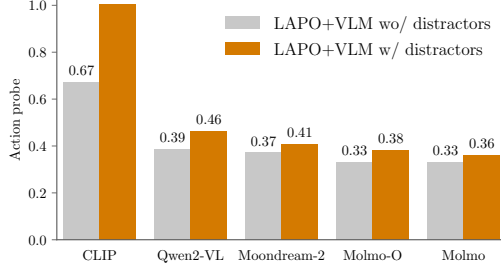


Figure 7: Molmo performance investigation, using aggregation over the best hyperparameters. We benchmark both Molmo versions, which both use CLIP but differ in LLM backbones (OLMo vs Qwen2), as well as Qwen2-VL. Since both Molmo share the pre-training data but differ in architecture, we conclude that the likely source of their superior performance lies in the data.

[34, 23, 26] using the same protocol as earlier, but separately as they require different prompt formats. As can be seen in Figure 6, such models do not deliver any substantial gains. In fact, VLM2Vec-V2 [34], best model in its class, performed worse than Gemma-3, which was the weakest model in the main benchmark, and none of the models surpassed Molmo. Our results indicate that embedding VLMs do not actually encode only prompt-specific visual information into the embeddings and fail to deliver the anticipated benefits.

Why does Molmo perform so well? Given Molmo’s strong performance, it is natural to ask what drives its improved representations. Directly answering this is difficult, but we can gather indirect evidence suggesting that the gains stem primarily from pre-training data rather than from the specific LLM or vision encoder architecture. Fortunately, Molmo provides two variants: Molmo-D, which uses Qwen2 as its backbone [50], and Molmo-O, which uses OLMo [22], while both employ CLIP [39] as the vision encoder. In contrast, Qwen2-VL [49] does not use CLIP, offering a useful comparison point to disentangle architectural effects. We therefore benchmarked and compared these models, as shown in Figure 7. The results show that CLIP alone performs the worst, Molmo-O ranks second after Molmo-D, and Qwen2-VL performs worse still. Since the Molmo variants share the same pre-training data but differ in backbone architecture, we conclude that the likely source of their superior performance lies in the data rather than the architecture. A further hypothesis is that Molmo’s advantage may come from its visual pointing abilities, but this seems unlikely since Moondream-2 also has this ability yet performs worse.

6 PROMPTABLE REPRESENTATIONS UNLOCK TASK-CENTRIC LATENT ACTIONS

Based on the benchmark results (see Figure 4), we selected multiple VLMs from worst to best for further experiments: Gemma-3, Phi-4, Molmo and GraspMolmo. **As an additional baseline we evaluated OTTER [24] approach to promptable representations.** Although all of them achieved improvements in latent action quality upon LAPO on small datasets, it remains necessary to validate whether this performance transfers to the full 5k datasets and yields improved success rates, as this is not guaranteed [36]. We chose the best hyperparameters for each VLM and trained LAPO+VLM on the full datasets, using three random seeds. As specified in Section 3 we used 16 labeled trajectories with ground-truth actions for final fine-tuning. See Section C for complete hyperparameters.

Results. We present the resulting action probes for each task in Figure 8 and final success rates after fine-tuning on 16 trajectories with real actions in Figure 9. As can be seen in Figure 8, LAPO+VLMs achieve a substantial improvement in latent action quality, both with and without distractors. With distractors, they nearly close the gap to LAPO trained without distractors, and without distractors, they slightly outperform it (e.g., Molmo). Note that we used the best hyperparameters, which can be

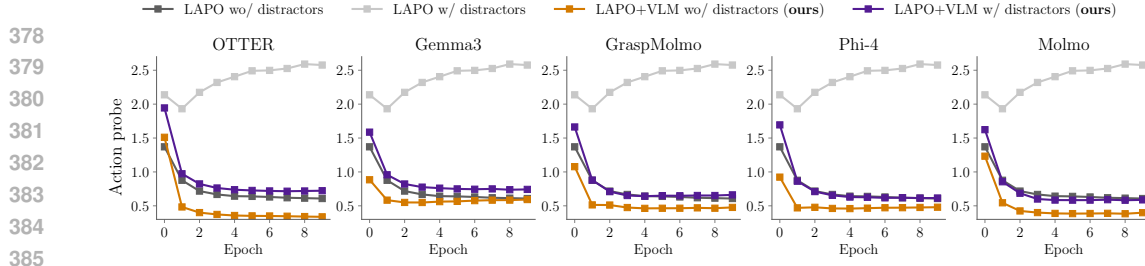


Figure 8: Action probes comparison for LAPO and LAPO+VLMs on full datasets for all tasks in MT10. Results are averaged over three random seeds. As can be seen, LAPO+VLMs significantly improves upon LAPO in terms of the latent actions quality, and without any supervision **with true actions** closes the gap with LAPO without distractors. While all VLMs bring improvements, Molmo achieve best results overall, especially given its high robustness to hyperparameter choices (see Figure 4a). For resulting success rates see Figure 9. We provide per-environment probes in Figure 13, Section A.

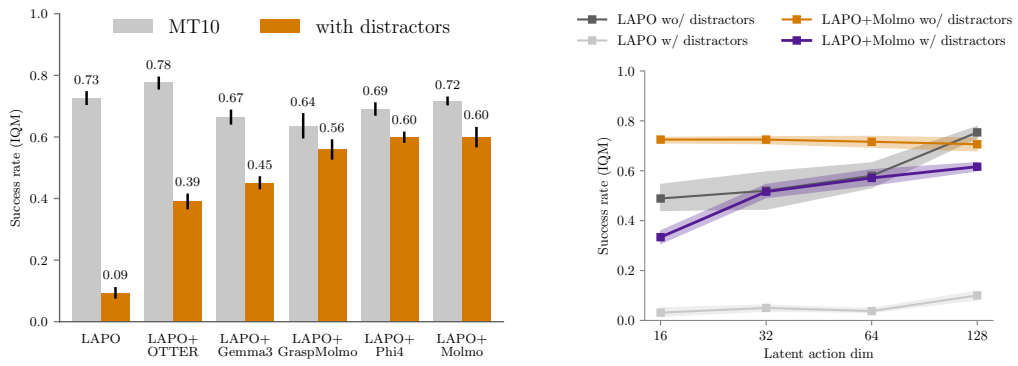


Figure 9: Success rate on MT10 for LAPO and LAPO+VLMs, which uses promptable representations. We use three random seeds and report IQM and 95%-CI based on stratified bootstrapping, following the Agarwal et al. [1].

Figure 10: Success rate on MT10 for LAPO and LAPO+Molmo, with varying latent action dimension to control the information bottleneck. We use three random seeds and report IQM and 95%-CI based on stratified bootstrapping, following the Agarwal et al. [1].

hard to find without ground-truth actions in real-world scenarios. Thus, the high robustness of Molmo to different hyperparameter choices (see Figure 4) is an important property for practical scenarios.

Crucially, the improvement in action probes on full datasets carries over to downstream performance (see Figure 9): success rates increase by a factor of six at max in the presence of distractors, while remaining almost unchanged without them. Interestingly, we found Phi-4 to outperform GraspMolmo, despite having worse probes on small datasets. On full datasets (Figure 8), however, Phi-4 is better. This indicates, that while results from a small dataset may carry over to a larger one with some error, probes on the full dataset predict the final success rate with high accuracy. **We also observe that OTTER’s [24] training-free promptable representation extraction from CLIP [39] performs worse than native VLMs such as Gemma3 or Molmo.** Overall our results confirm the viability of promptable representations as a clean target for latent action modeling under distracting conditions.

Varying the latent action information bottleneck. In all previous experiments, we fixed the latent action dimension to 128 to ensure the same level of latent action minimality across all methods. However, 128 was inherited from LAPO and may not be optimal. Therefore, we conducted additional experiments varying the latent action dimension, using full datasets and three random seeds. The results are summarized in Figure 10. We observe that promptable representations not only increase success rates in the presence of distractors but also significantly improve upon LAPO without distractors under stronger minimality constraints (e.g. 16 action dimensions). This further supports the claim that VLMs help filter out information that is not relevant to controllable changes, allowing for more compact latent action space.

432 7 DISCUSSION AND LIMITATIONS

434 **Segmentation, while simple, is not enough.** The concept of extracting VLM embeddings with the
 435 hope that they will filter out distractors may initially seem strange. If the goal is to filter out distractors,
 436 would not it be more straightforward to simply segment the relevant parts and train LAPO directly in
 437 image space using masks? In fact, our benchmark includes VLMs capable of segmentation, such as
 438 Sa2VA [55], and we even utilize such prompts (see Table 1), yet we still rely on embeddings instead
 439 of masks. While segmentation is appealing, it does not address the fundamental problem. Consider a
 440 scenario with a robotic arm and varying lighting conditions. Even if we segment the arm, we will
 441 still get changes in our observations that are not related to the actual actions, such as color shifts and
 442 reflections on the arm. The same issue arises with camera movement and changes in perspective. The
 443 key, therefore, is to work in a semantic latent space, which is where the common-sense reasoning
 444 capabilities of VLMs become crucial.

445 **On the choice of MetaWorld benchmark.** One notable limitation of our study is its small scale,
 446 as we rely on MetaWorld as our primary benchmark and do not extend our analysis to large VLAs
 447 and datasets, such as Open-X [38]. However, this choice is deliberate for two reasons. First, while
 448 MetaWorld is simple, with distractors, it is difficult enough to completely break traditional LAMs and
 449 to distinguish different VLMs in terms of the promptable representations’ quality (as we demonstrate
 450 in Section 5). As an early exploration, it was crucial to expand in variety (e.g., exploring more VLMs)
 451 within our limited resources. We hope that our analysis provides practitioners with valuable insights
 452 into the available options. Second, encoding entire datasets is both expensive and time-consuming,
 453 as it involves inference with large VLMs (e.g., 8B parameters) and generating answers. For our 5k
 454 trajectory datasets, the process can quickly exceed 24 hours, let alone for truly large datasets. Since
 455 this is purely inference and gradients are not required, the process can be significantly accelerated,
 456 for example, using vLLM [29]. However, we have left this as future work.

457 8 RELATED WORK

459 **Latent action learning.** Imitating policy given only observations is the problem that latent action
 460 learning tries to tackle. Edwards et al. [17] suggested extracting latent actions from consecutive
 461 states with the help of some amount of true actions present. LAPO [42] scales up the approach
 462 by introducing a bottleneck between forward and backward dynamics. Building on LAPO, other
 463 approaches emerged that continued to scale latent action extraction for pre-training action models
 464 [5, 7, 58, 6, 25]. However, most of the above methods imply the presence of either noise-free datasets
 465 or an abundance of ground-truth action labels, which in general is not true for in-the-wild video data
 466 Grauman et al. [20; 21].

467 Some of the previous works Nikulin et al. [36], Zhang et al. [56] show that, with noise, the quality of
 468 latent actions degrades promptly, and the only proposed remedy was to increase the number of action
 469 labels. In our work, we propose a way to extract latent actions that is robust to exogenous noise and,
 470 at the same time, does not require true action labels.

471 **Promptable representations.** In contrast to state augmentation techniques, code generation, or
 472 reward modeling [3, 48, 15], the approach of promptable representations uses the internal embeddings
 473 of large models for performing a downstream task. Chen et al. [9] use VLM embeddings generated
 474 with a task-specific prompt to extract better state representations. Using them as input, it enhances the
 475 performance of an RL model both in Minecraft and Habitat environments. Similar work by Huang
 476 et al. [24] also employs semantic extraction by using a dot product of text and visual features from
 477 CLIP, which allows for claiming superior performance of an action model on robotic benchmarks.
 478 The important difference must be emphasized: both aforementioned works use VLM to *enhance* the
 479 performance of downstream algorithms. In contrast, when exogenous noise is present in the data, the
 480 quality of latent actions is exponentially worse [35] (than without the noise). Thus, filtering the noise
 481 with the common-sense abilities of VLMs is a way to make Latent Action Models show reasonable
 482 performance.

483 There exists another approach, UniVLA [8], aimed at task-specific latent action filtering. **UniVLA**
 484 **adds the language task instruction embedding to the IDM and FDM inputs, which may help disentangle**
 485 **task-relevant videos from noise at a high level, but does not provide the per-step learning signal**
 486 **needed to accurately recover low-level ground-truth actions. As a result, during single-task learning**

486 the task instruction is a constant vector, and UniVLA effectively reduces to LAPO. This is a general
 487 limitation of UniVLA, whereas we show that promptable representations remain effective even in the
 488 single-task learning regime.
 489

490 9 CONCLUSION

492 In this work, we demonstrated that promptable representations provided by Vision-Language Models
 493 can effectively filter out action-correlated distractors, enabling task-centric latent actions. Our ex-
 494 periments on the Distracting MetaWorld benchmark confirmed that using task-centric promptable
 495 representations as targets for LAPO substantially improves both latent action quality and down-
 496 stream success rates. We hope that our results will inspire the community to explore promptable
 497 representations at scale for the next generation of Vision-Language-Action models.
 498

499 REFERENCES

501 [1] Rishabh Agarwal, Max Schwarzer, Pablo Samuel Castro, Aaron C Courville, and Marc Belle-
 502 mare. Deep reinforcement learning at the edge of the statistical precipice. *Advances in neural*
 503 *information processing systems*, 34:29304–29320, 2021.

504 [2] Pravesh Agrawal, Szymon Antoniak, Emma Bou Hanna, Baptiste Bout, Devendra Chaplot,
 505 Jessica Chudnovsky, Diogo Costa, Baudouin De Moncault, Saurabh Garg, Theophile Gervet,
 506 et al. Pixtral 12b. *arXiv preprint arXiv:2410.07073*, 2024.

508 [3] Michael Ahn, Anthony Brohan, Noah Brown, Yevgen Chebotar, Omar Cortes, Byron David,
 509 Chelsea Finn, Chuyuan Fu, Keerthana Gopalakrishnan, Karol Hausman, et al. Do as i can, not
 510 as i say: Grounding language in robotic affordances. *arXiv preprint arXiv:2204.01691*, 2022.

511 [4] Alisson Azzolini, Junjie Bai, Hannah Brandon, Jiaxin Cao, Prithvijit Chattopadhyay, Huayu
 512 Chen, Jinju Chu, Yin Cui, Jenna Diamond, Yifan Ding, et al. Cosmos-reason1: From physical
 513 common sense to embodied reasoning. *arXiv preprint arXiv:2503.15558*, 2025.

515 [5] Johan Bjorck, Fernando Castañeda, Nikita Cherniadev, Xingye Da, Runyu Ding, Linxi Fan,
 516 Yu Fang, Dieter Fox, Fengyuan Hu, Spencer Huang, et al. Gr00t n1: An open foundation model
 517 for generalist humanoid robots. *arXiv preprint arXiv:2503.14734*, 2025.

518 [6] Jake Bruce, Michael D Dennis, Ashley Edwards, Jack Parker-Holder, Yuge Shi, Edward Hughes,
 519 Matthew Lai, Aditi Mavalankar, Richie Steigerwald, Chris Apps, et al. Genie: Generative
 520 interactive environments. In *Forty-first International Conference on Machine Learning*, 2024.

522 [7] Qingwen Bu, Jisong Cai, Li Chen, Xiuqi Cui, Yan Ding, Siyuan Feng, Shenyuan Gao, Xindong
 523 He, Xuan Hu, Xu Huang, et al. Agibot world colosseo: A large-scale manipulation platform for
 524 scalable and intelligent embodied systems. *arXiv preprint arXiv:2503.06669*, 2025.

525 [8] Qingwen Bu, Yanting Yang, Jisong Cai, Shenyuan Gao, Guanghui Ren, Maoqing Yao, Ping
 526 Luo, and Hongyang Li. Univla: Learning to act anywhere with task-centric latent actions, 2025.
 527 URL <https://arxiv.org/abs/2505.06111>.

529 [9] William Chen, Oier Mees, Aviral Kumar, and Sergey Levine. Vision-language models provide
 530 promptable representations for reinforcement learning. *arXiv preprint arXiv:2402.02651*, 2024.

531 [10] Xiaoyu Chen, Junliang Guo, Tianyu He, Chuheng Zhang, Pushi Zhang, Derek Cathera Yang,
 532 Li Zhao, and Jiang Bian. Igor: Image-goal representations are the atomic control units for
 533 foundation models in embodied ai. *arXiv preprint arXiv:2411.00785*, 2024.

535 [11] Yi Chen, Yuying Ge, Yizhuo Li, Yixiao Ge, Mingyu Ding, Ying Shan, and Xihui Liu.
 536 Moto: Latent motion token as the bridging language for robot manipulation. *arXiv preprint*
 537 *arXiv:2412.04445*, 2024.

538 [12] Zichen Jeff Cui, Hengkai Pan, Aadhithya Iyer, Siddhant Haldar, and Lerrel Pinto. Dynamo:
 539 In-domain dynamics pretraining for visuo-motor control. *arXiv preprint arXiv:2409.12192*,
 2024.

540 [13] Yasser Dahou, Ngoc Dung Huynh, Phuc H Le-Khac, Wamiq Reyaz Para, Ankit Singh,
 541 and Sanath Narayan. Vision-language models can't see the obvious. *arXiv preprint*
 542 *arXiv:2507.04741*, 2025.

543 [14] Wenliang Dai, Junnan Li, Dongxu Li, Anthony Tiong, Junqi Zhao, Weisheng Wang, Boyang Li,
 544 Pascale N Fung, and Steven Hoi. Instructblip: Towards general-purpose vision-language models
 545 with instruction tuning. *Advances in neural information processing systems*, 36:49250–49267,
 546 2023.

547 [15] Nitish Dashora, Dibya Ghosh, and Sergey Levine. Viva: Video-trained value functions for guid-
 548 ing online rl from diverse data, 2025. URL <https://arxiv.org/abs/2503.18210>.

549 [16] Matt Deitke, Christopher Clark, Sangho Lee, Rohun Tripathi, Yue Yang, Jae Sung Park,
 550 Mohammadreza Salehi, Niklas Muennighoff, Kyle Lo, Luca Soldaini, et al. Molmo and pixmo:
 551 Open weights and open data for state-of-the-art vision-language models. In *Proceedings of the*
 552 *Computer Vision and Pattern Recognition Conference*, pp. 91–104, 2025.

553 [17] Ashley Edwards, Himanshu Sahni, Yannick Schroecker, and Charles Isbell. Imitating latent
 554 policies from observation. In *International conference on machine learning*, pp. 1755–1763.
 555 PMLR, 2019.

556 [18] Shenyuan Gao, Siyuan Zhou, Yilun Du, Jun Zhang, and Chuang Gan. Adaworld: Learning
 557 adaptable world models with latent actions. *arXiv preprint arXiv:2503.18938*, 2025.

558 [19] Chenhui Gou, Abdulwahab Felemban, Faizan Farooq Khan, Deyao Zhu, Jianfei Cai, Hamid
 559 Rezatofighi, and Mohamed Elhoseiny. How well can vision language models see image details?
 560 *arXiv preprint arXiv:2408.03940*, 2024.

561 [20] Kristen Grauman, Andrew Westbury, Eugene Byrne, Zachary Chavis, Antonino Furnari, Rohit
 562 Girdhar, Jackson Hamburger, Hao Jiang, Miao Liu, Xingyu Liu, Miguel Martin, Tushar Nagarajan,
 563 Ilija Radosavovic, Santhosh Kumar Ramakrishnan, Fiona Ryan, Jayant Sharma, Michael
 564 Wray, Mengmeng Xu, Eric Zhongcong Xu, Chen Zhao, Siddhant Bansal, Dhruv Batra, Vincent
 565 Cartillier, Sean Crane, Tien Do, Morrie Doulaty, Akshay Erapalli, Christoph Feichtenhofer,
 566 Adriano Fragomeni, Qichen Fu, Abrham Gebreselasie, Cristina Gonzalez, James Hillis, Xuhua
 567 Huang, Yifei Huang, Wenqi Jia, Leslie Khoo, Jachym Kolar, Satwik Kottur, Anurag Kumar,
 568 Federico Landini, Chao Li, Yanghao Li, Zhenqiang Li, Karttikay Mangalam, Raghava Mod-
 569 hugu, Jonathan Munro, Tullie Murrell, Takumi Nishiyasu, Will Price, Paola Ruiz Puentes, Merey
 570 Ramazanova, Leda Sari, Kiran Somasundaram, Audrey Southerland, Yusuke Sugano, Ruijie
 571 Tao, Minh Vo, Yuchen Wang, Xindi Wu, Takuma Yagi, Ziwei Zhao, Yunyi Zhu, Pablo Arbelaez,
 572 David Crandall, Dima Damen, Giovanni Maria Farinella, Christian Fuegen, Bernard Ghanem,
 573 Vamsi Krishna Ithapu, C. V. Jawahar, Hanbyul Joo, Kris Kitani, Haizhou Li, Richard Newcombe,
 574 Aude Oliva, Hyun Soo Park, James M. Rehg, Yoichi Sato, Jianbo Shi, Mike Zheng Shou, Antonio
 575 Torralba, Lorenzo Torresani, Mingfei Yan, and Jitendra Malik. Ego4d: Around the world in
 576 3,000 hours of egocentric video, 2022. URL <https://arxiv.org/abs/2110.07058>.

577 [21] Kristen Grauman, Andrew Westbury, Lorenzo Torresani, Kris Kitani, Jitendra Malik, Tri-
 578 antafyllos Afouras, Kumar Ashutosh, Vijay Baiyya, Siddhant Bansal, Bikram Boote, Eugene
 579 Byrne, Zach Chavis, Joya Chen, Feng Cheng, Fu-Jen Chu, Sean Crane, Avijit Dasgupta, Jing
 580 Dong, Maria Escobar, Cristhian Forigua, Abrham Gebreselasie, Sanjay Haresh, Jing Huang,
 581 Md Mohaiminul Islam, Suyog Jain, Rawal Khirodkar, Devansh Kukreja, Kevin J Liang, Jia-Wei
 582 Liu, Sagnik Majumder, Yongsen Mao, Miguel Martin, Effrosyni Mavroudi, Tushar Nagarajan,
 583 Francesco Ragusa, Santhosh Kumar Ramakrishnan, Luigi Seminara, Arjun Somayazulu, Yale
 584 Song, Shan Su, Zihui Xue, Edward Zhang, Jinxu Zhang, Angela Castillo, Changan Chen, Xinzhu
 585 Fu, Ryosuke Furuta, Cristina Gonzalez, Prince Gupta, Jiabo Hu, Yifei Huang, Yiming Huang,
 586 Leslie Khoo, Anush Kumar, Robert Kuo, Sach Lakhavani, Miao Liu, Mi Luo, Zhengyi Luo,
 587 Brighid Meredith, Austin Miller, Oluwatumini Oguntola, Xiaqing Pan, Penny Peng, Shraman
 588 Pramanick, Merey Ramazanova, Fiona Ryan, Wei Shan, Kiran Somasundaram, Chenan Song,
 589 Audrey Southerland, Masatoshi Tateno, Huiyu Wang, Yuchen Wang, Takuma Yagi, Mingfei Yan,
 590 Xitong Yang, Zecheng Yu, Shengxin Cindy Zha, Chen Zhao, Ziwei Zhao, Zhifan Zhu, Jeff Zhuo,
 591 Pablo Arbelaez, Gedas Bertasius, David Crandall, Dima Damen, Jakob Engel, Giovanni Maria
 592 Farinella, Antonino Furnari, Bernard Ghanem, Judy Hoffman, C. V. Jawahar, Richard New-
 593 combe, Hyun Soo Park, James M. Rehg, Yoichi Sato, Manolis Savva, Jianbo Shi, Mike Zheng

594 Shou, and Michael Wray. Ego-exo4d: Understanding skilled human activity from first- and
 595 third-person perspectives, 2024. URL <https://arxiv.org/abs/2311.18259>.

596

597 [22] Dirk Groeneveld, Iz Beltagy, Pete Walsh, Akshita Bhagia, Rodney Kinney, Oyvind Tafjord,
 598 Ananya Harsh Jha, Hamish Ivison, Ian Magnusson, Yizhong Wang, et al. Olmo: Accelerating
 599 the science of language models. *arXiv preprint arXiv:2402.00838*, 2024.

600 [23] Tiancheng Gu, Kaicheng Yang, Ziyong Feng, Xingjun Wang, Yanzhao Zhang, Dingkun Long,
 601 Yingda Chen, Weidong Cai, and Jiankang Deng. Breaking the modality barrier: Universal
 602 embedding learning with multimodal llms. *arXiv preprint arXiv:2504.17432*, 2025.

603

604 [24] Huang Huang, Fangchen Liu, Letian Fu, Tingfan Wu, Mustafa Mukadam, Jitendra Malik, Ken
 605 Goldberg, and Pieter Abbeel. Otter: A vision-language-action model with text-aware visual
 606 feature extraction. *arXiv preprint arXiv:2503.03734*, 2025.

607 [25] Joel Jang, Seonghyeon Ye, Zongyu Lin, Jiannan Xiang, Johan Bjorck, Yu Fang, Fengyuan Hu,
 608 Spencer Huang, Kaushil Kundalia, Yen-Chen Lin, et al. Dreamgen: Unlocking generalization
 609 in robot learning through video world models. *arXiv preprint arXiv:2505.12705*, 2025.

610

611 [26] Ting Jiang, Minghui Song, Zihan Zhang, Haizhen Huang, Weiwei Deng, Feng Sun, Qi Zhang,
 612 Deqing Wang, and Fuzhen Zhuang. E5-v: Universal embeddings with multimodal large
 613 language models. *arXiv preprint arXiv:2407.12580*, 2024.

614

615 [27] Ziyan Jiang, Rui Meng, Xinyi Yang, Semih Yavuz, Yingbo Zhou, and Wenhui Chen. Vlm2vec:
 616 Training vision-language models for massive multimodal embedding tasks. *arXiv preprint
 617 arXiv:2410.05160*, 2024.

618

619 [28] Albina Klepacch, Alexander Nikulin, Ilya Zisman, Denis Tarasov, Alexander Derevyagin, Andrei
 620 Polubarov, Nikita Lyubaykin, and Vladislav Kurenkov. Object-centric latent action learning.
 621 *arXiv preprint arXiv:2502.09680*, 2025.

622

623 [29] Woosuk Kwon, Zhuohan Li, Siyuan Zhuang, Ying Sheng, Lianmin Zheng, Cody Hao Yu,
 624 Joseph Gonzalez, Hao Zhang, and Ion Stoica. Efficient memory management for large language
 625 model serving with pagedattention. In *Proceedings of the 29th symposium on operating systems
 626 principles*, pp. 611–626, 2023.

627

628 [30] Wenyan Li, Raphael Tang, Chengzu Li, Caiqi Zhang, Ivan Vulić, and Anders Søgaard. Lost in
 629 embeddings: Information loss in vision-language models. *arXiv preprint arXiv:2509.11986*,
 630 2025.

631

632 [31] Anthony Liang, Pavel Czempin, Matthew Hong, Yutai Zhou, Erdem Biyik, and Stephen Tu.
 633 Clam: Continuous latent action models for robot learning from unlabeled demonstrations. *arXiv
 634 preprint arXiv:2505.04999*, 2025.

635

636 [32] YuXuan Liu, Abhishek Gupta, Pieter Abbeel, and Sergey Levine. Imitation from observation:
 637 Learning to imitate behaviors from raw video via context translation. In *2018 IEEE international
 638 conference on robotics and automation (ICRA)*, pp. 1118–1125. IEEE, 2018.

639

640 [33] Robert McCarthy, Daniel CH Tan, Dominik Schmidt, Fernando Acero, Nathan Herr, Yilun Du,
 641 Thomas G Thuruthel, and Zhibin Li. Towards generalist robot learning from internet video: A
 642 survey. *Journal of Artificial Intelligence Research*, 83, 2025.

643

644 [34] Rui Meng, Ziyan Jiang, Ye Liu, Mingyi Su, Xinyi Yang, Yuepeng Fu, Can Qin, Zeyuan Chen,
 645 Ran Xu, Caiming Xiong, et al. Vlm2vec-v2: Advancing multimodal embedding for videos,
 646 images, and visual documents. *arXiv preprint arXiv:2507.04590*, 2025.

647

648 [35] Dipendra Misra, Akanksha Saran, Tengyang Xie, Alex Lamb, and John Langford. Towards
 649 principled representation learning from videos for reinforcement learning, 2024. URL <https://arxiv.org/abs/2403.13765>.

650

651 [36] Alexander Nikulin, Ilya Zisman, Denis Tarasov, Nikita Lyubaykin, Andrei Polubarov, Igor
 652 Kiselev, and Vladislav Kurenkov. Latent action learning requires supervision in the presence of
 653 distractors. *arXiv preprint arXiv:2502.00379*, 2025.

648 [37] Maxime Oquab, Timothée Darzet, Théo Moutakanni, Huy Vo, Marc Szafraniec, Vasil Khalidov,
 649 Pierre Fernandez, Daniel Haziza, Francisco Massa, Alaaeldin El-Nouby, et al. Dinov2: Learning
 650 robust visual features without supervision. *arXiv preprint arXiv:2304.07193*, 2023.

651
 652 [38] Abby O'Neill, Abdul Rehman, Abhiram Maddukuri, Abhishek Gupta, Abhishek Padalkar,
 653 Abraham Lee, Acorn Pooley, Agrim Gupta, Ajay Mandlekar, Ajinkya Jain, et al. Open x-
 654 embodiment: Robotic learning datasets and rt-x models: Open x-embodiment collaboration 0.
 655 In *2024 IEEE International Conference on Robotics and Automation (ICRA)*, pp. 6892–6903.
 656 IEEE, 2024.

657 [39] Alec Radford, Jong Wook Kim, Chris Hallacy, Aditya Ramesh, Gabriel Goh, Sandhini Agarwal,
 658 Girish Sastry, Amanda Askell, Pamela Mishkin, Jack Clark, et al. Learning transferable visual
 659 models from natural language supervision. In *International conference on machine learning*,
 660 pp. 8748–8763. PMLR, 2021.

661 [40] Pooyan Rahmazadehgervi, Logan Bolton, Mohammad Reza Taesiri, and Anh Totti Nguyen.
 662 Vision language models are blind: Failing to translate detailed visual features into words. *arXiv
 663 preprint arXiv:2407.06581*, 2024.

664 [41] Oleh Rybkin, Karl Pertsch, Konstantinos G Derpanis, Kostas Daniilidis, and Andrew Jaegle.
 665 Learning what you can do before doing anything. *arXiv preprint arXiv:1806.09655*, 2018.

666 [42] Dominik Schmidt and Minqi Jiang. Learning to act without actions. *arXiv preprint
 667 arXiv:2312.10812*, 2023.

668 [43] Mong Yuan Sim, Wei Emma Zhang, Xiang Dai, and Biaoyan Fang. Can VLMs actually
 669 see and read? a survey on modality collapse in vision-language models. In Wanxiang Che,
 670 Joyce Nabende, Ekaterina Shutova, and Mohammad Taher Pilehvar (eds.), *Findings of the
 671 Association for Computational Linguistics: ACL 2025*, pp. 24452–24470, Vienna, Austria, July
 672 2025. Association for Computational Linguistics. ISBN 979-8-89176-256-5. doi: 10.18653/v1/
 673 2025.findings-acl.1256. URL [https://aclanthology.org/2025.findings-acl.
 674 1256/](https://aclanthology.org/2025.findings-acl.1256/).

675 [44] Austin Stone, Oscar Ramirez, Kurt Konolige, and Rico Jonschkowski. The distracting con-
 676 trol suite—a challenging benchmark for reinforcement learning from pixels. *arXiv preprint
 677 arXiv:2101.02722*, 2021.

678 [45] Gemma Team, Aishwarya Kamath, Johan Ferret, Shreya Pathak, Nino Vieillard, Ramona
 679 Merhej, Sarah Perrin, Tatiana Matejovicova, Alexandre Ramé, Morgane Rivière, et al. Gemma
 680 3 technical report. *arXiv preprint arXiv:2503.19786*, 2025.

681 [46] Faraz Torabi, Garrett Warnell, and Peter Stone. Recent advances in imitation learning from
 682 observation. *arXiv preprint arXiv:1905.13566*, 2019.

683 [47] Ashish Vaswani, Noam Shazeer, Niki Parmar, Jakob Uszkoreit, Llion Jones, Aidan N Gomez,
 684 Łukasz Kaiser, and Illia Polosukhin. Attention is all you need. *Advances in neural information
 685 processing systems*, 30, 2017.

686 [48] Boyuan Wang, Yun Qu, Yuhang Jiang, Jianzhun Shao, Chang Liu, Wenming Yang, and Xi-
 687 angyang Ji. Llm-empowered state representation for reinforcement learning, 2024. URL
 688 <https://arxiv.org/abs/2407.13237>.

689 [49] Peng Wang, Shuai Bai, Sinan Tan, Shijie Wang, Zhihao Fan, Jinze Bai, Keqin Chen, Xuejing
 690 Liu, Jialin Wang, Wenbin Ge, et al. Qwen2-vl: Enhancing vision-language model's perception
 691 of the world at any resolution. *arXiv preprint arXiv:2409.12191*, 2024.

692 [50] An Yang, Anfeng Li, Baosong Yang, Beichen Zhang, Binyuan Hui, Bo Zheng, Bowen Yu,
 693 Chang Gao, Chengan Huang, Chenxu Lv, et al. Qwen3 technical report. *arXiv preprint
 694 arXiv:2505.09388*, 2025.

695 [51] Jiange Yang, Yansong Shi, Haoyi Zhu, Mingyu Liu, Kaijing Ma, Yating Wang, Gangshan Wu,
 696 Tong He, and Limin Wang. Como: Learning continuous latent motion from internet videos for
 697 scalable robot learning. *arXiv preprint arXiv:2505.17006*, 2025.

702 [52] Ruihan Yang, Qinxi Yu, Yecheng Wu, Rui Yan, Borui Li, An-Chieh Cheng, Xueyan Zou,
 703 Yunhao Fang, Hongxu Yin, Sifei Liu, et al. Egovla: Learning vision-language-action models
 704 from egocentric human videos. *arXiv preprint arXiv:2507.12440*, 2025.

705 [53] Seonghyeon Ye, Joel Jang, Byeongguk Jeon, Sejune Joo, Jianwei Yang, Baolin Peng, Ajay
 706 Mandlekar, Reuben Tan, Yu-Wei Chao, Bill Yuchen Lin, et al. Latent action pretraining from
 707 videos. *arXiv preprint arXiv:2410.11758*, 2024.

709 [54] Tianhe Yu, Deirdre Quillen, Zhanpeng He, Ryan Julian, Karol Hausman, Chelsea Finn, and
 710 Sergey Levine. Meta-world: A benchmark and evaluation for multi-task and meta reinforcement
 711 learning. In *Conference on robot learning*, pp. 1094–1100. PMLR, 2020.

712 [55] Haobo Yuan, Xiangtai Li, Tao Zhang, Zilong Huang, Shilin Xu, Shunping Ji, Yunhai Tong,
 713 Lu Qi, Jiashi Feng, and Ming-Hsuan Yang. Sa2va: Marrying sam2 with llava for dense grounded
 714 understanding of images and videos. *arXiv preprint arXiv:2501.04001*, 2025.

716 [56] Chuheng Zhang, Tim Pearce, Pushi Zhang, Kaixin Wang, Xiaoyu Chen, Wei Shen, Li Zhao,
 717 and Jiang Bian. What do latent action models actually learn? *arXiv preprint arXiv:2506.15691*,
 718 2025.

719 [57] Qinqing Zheng, Mikael Henaff, Brandon Amos, and Aditya Grover. Semi-supervised offline
 720 reinforcement learning with action-free trajectories. In *International conference on machine
 721 learning*, pp. 42339–42362. PMLR, 2023.

723 [58] Yifan Zhong, Fengshuo Bai, Shaofei Cai, Xuchuan Huang, Zhang Chen, Xiaowei Zhang,
 724 Yuanfei Wang, Shaoyang Guo, Tianrui Guan, Ka Nam Lui, et al. A survey on vision-language-
 725 action models: An action tokenization perspective. *arXiv preprint arXiv:2507.01925*, 2025.

726
 727
 728
 729
 730
 731
 732
 733
 734
 735
 736
 737
 738
 739
 740
 741
 742
 743
 744
 745
 746
 747
 748
 749
 750
 751
 752
 753
 754
 755

A ADDITIONAL FIGURES

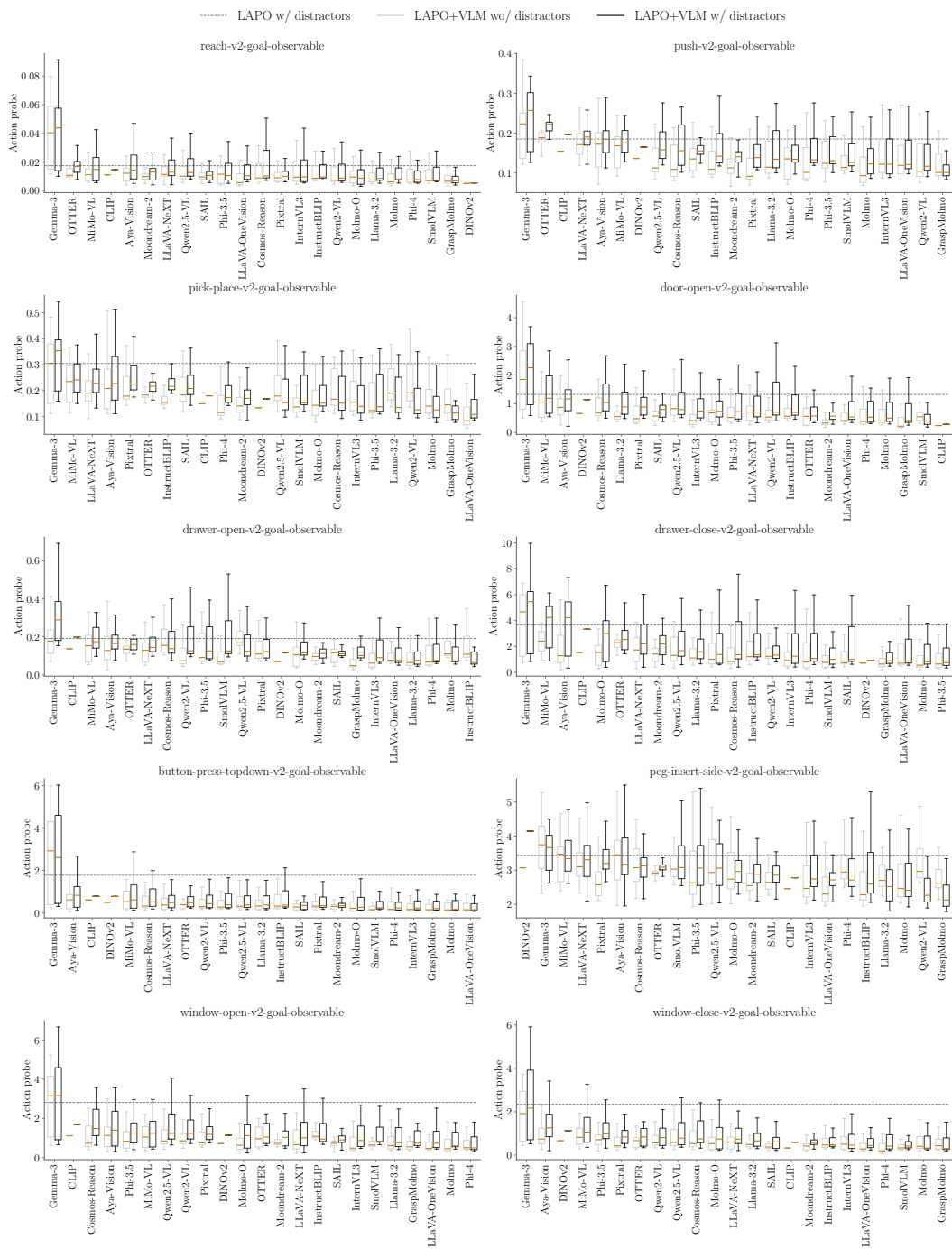


Figure 11: Aggregation over all hyperparameters for each task in MT10.

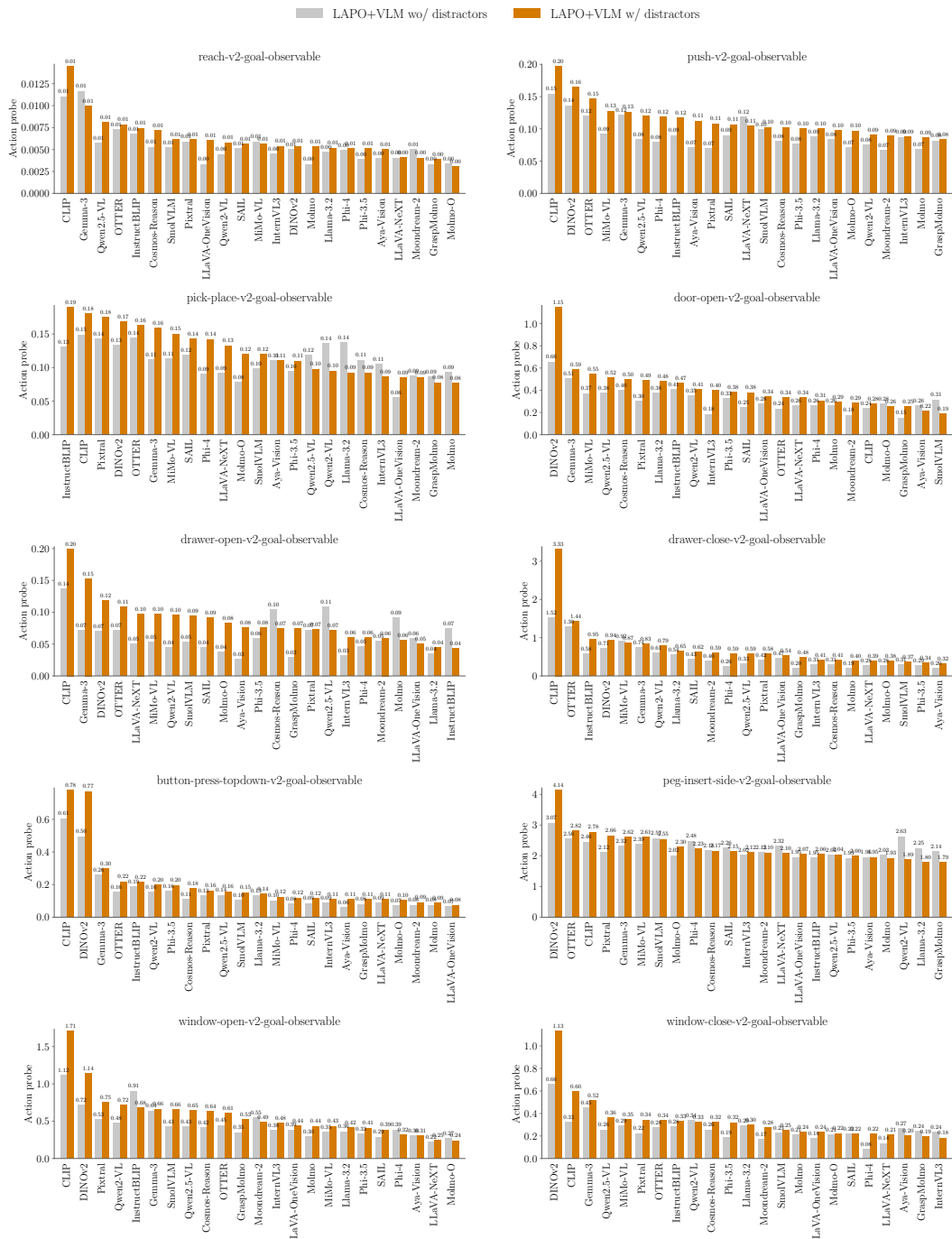


Figure 12: Probe values for best hyperparameters for each task in MT10.

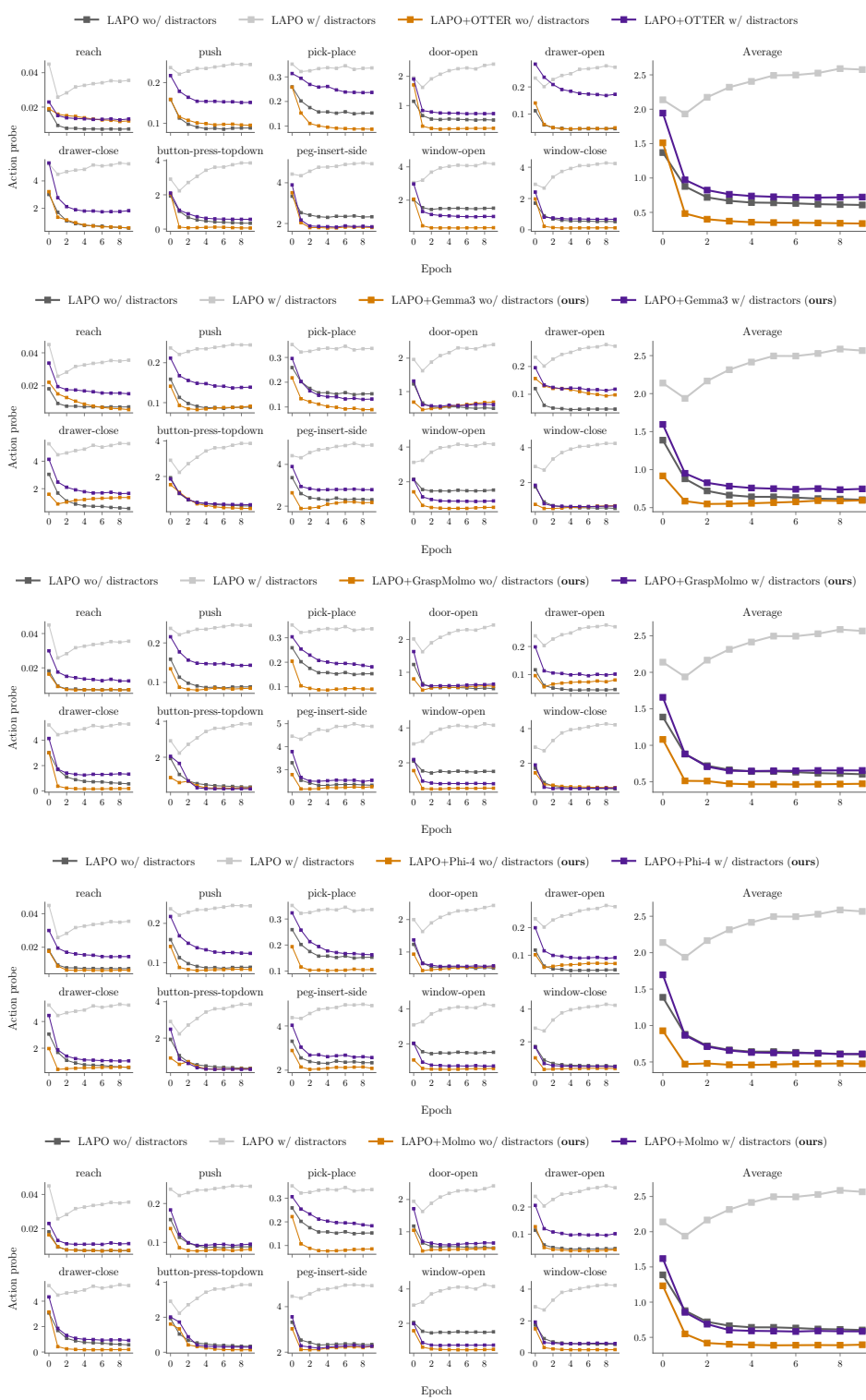
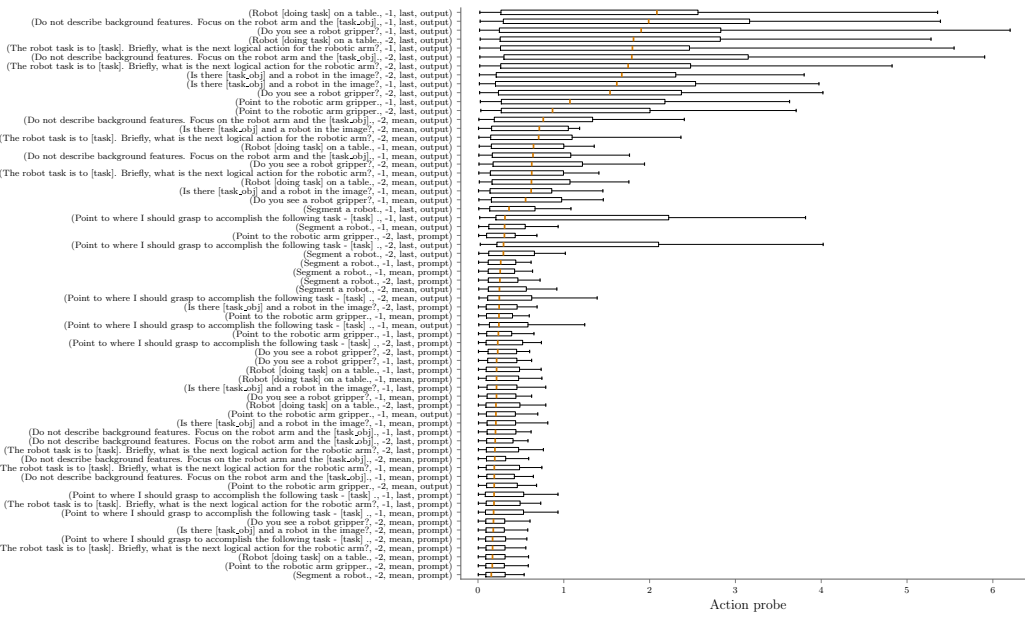


Figure 13: Action probes comparison for LAPO and LAPO+VLMs on full datasets for all tasks in MT10. Results are averaged over three random seeds. As can be seen, LAPO+VLM significantly improves upon LAPO in terms of the latent actions quality, and without any supervision **with true actions** closes the gap with LAPO without distractors. While all VLMs bring improvements, Molmo achieve best results overall. For resulting success rates see Figure 9

918
919
920
921
922
923
924
925
926
927
928
929
930
931
932
933



934 (Do not describe background features. Focus on the robotic arm and the [task,obj]. -1, last, output) |
935 (The robot task is to [task]. Briefly, what is the next logical action for the robotic arm? -1, last, output) |
936 (Do not describe background features. Focus on the robotic arm and the [task,obj]. -2, last, output) |
937 (Do not describe background features. Focus on the robotic arm and the [task,obj]. -1, mean, output) |
938 (Do not describe background features. Focus on the robotic arm and the [task,obj]. -1, mean, output) |
939 (The robot task is to [task]. Briefly, what is the next logical action for the robotic arm? -1, mean, output) |
940 (Point to where I should grasp to accomplish the following task: [task]. -1, last, output) |
941 (Point to where I should grasp to accomplish the following task: [task]. -2, last, output) |
942 (Segment a robot. -1, last, output) |
943 (Point to where I should grasp to accomplish the following task: [task]. -2, last, output) |
944 (Point to where I should grasp to accomplish the following task: [task]. -1, mean, output) |
945 (Point to where I should grasp to accomplish the following task: [task]. -1, mean, output) |
946 (Do not describe background features. Focus on the robotic arm and the [task,obj]. -1, mean, output) |
947 (Do not describe background features. Focus on the robotic arm and the [task,obj]. -1, last, output) |
948 (The robot task is to [task]. Briefly, what is the next logical action for the robotic arm? -1, last, output) |
949 (Do not describe background features. Focus on the robotic arm and the [task,obj]. -1, mean, output) |
950 (Point to where I should grasp to accomplish the following task: [task]. -1, last, output) |
951 (Point to where I should grasp to accomplish the following task: [task]. -2, mean, output) |
952 (The robot task is to [task]. Briefly, what is the next logical action for the robotic arm? -2, mean, output) |
953 (Point to the robotic arm gripper. -1, mean, output) |
954 (Point to the robotic arm gripper. -2, mean, output) |
955 (Point to the robotic arm gripper. -1, mean, output) |
956 (Point to the robotic arm gripper. -2, mean, output) |
957 (Point to the robotic arm gripper. -1, mean, output) |
958 (Point to the robotic arm gripper. -2, mean, output) |
959 (Point to the robotic arm gripper. -1, mean, output) |
960 (Point to the robotic arm gripper. -2, mean, output) |
961 (Point to the robotic arm gripper. -1, mean, output) |
962 (Point to the robotic arm gripper. -2, mean, output) |
963 (Point to the robotic arm gripper. -1, mean, output) |
964 (Point to the robotic arm gripper. -2, mean, output) |
965 (Point to the robotic arm gripper. -1, mean, output) |
966 (Point to the robotic arm gripper. -2, mean, output) |
967 (Point to the robotic arm gripper. -1, mean, output) |
968 (Point to the robotic arm gripper. -2, mean, output) |
969 (Point to the robotic arm gripper. -1, mean, output) |
970 (Point to the robotic arm gripper. -2, mean, output) |
971

972 **B VISION-LANGUAGE MODELS DETAILS**
973

974 Table 1: Prompt templates used in our experiments. We adapt them to each task by inserting
975 information relevant to the task. All VLMs explored share the same prompts per task.
976

977

978 **Prompt**
979 The robot task is to [task]. Briefly, what is the next logical action for the robotic arm?
980 Do not describe background features. Focus on the robot arm and the [task-obj].
981 Do you see a robot gripper?
982 Is there [task-obj] and a robot in the image?
983 Robot [doing task] on a table.
984 Point to the robotic arm gripper.
985 Point to where I should grasp to accomplish the following task - [task].
986 Segment a robot.
987

988 Table 2: Exact HuggingFace IDs for all VLMs we used. We shortened their names in Figures to save
989 some space.
990

991

992 **Name** | **HuggingFace ID**
993

994 InstructBLIP | Salesforce/instructblip-vicuna-7b
995 Molmo | allenai/Molmo-7B-D-0924
996 Gemma-3 | google/gemma-3-12b-it
997 Llama-3.2 | unsloth/Llama-3.2-11B-Vision-Instruct
998 Qwen2.5-VL | Qwen/Qwen2.5-VL-7B-Instruct
999 InternVL3 | OpenGVLab/InternVL3-8B
1000 Cosmos-Reason | nvidia/Cosmos-Reason1-7B
1001 Phi-4 | microsoft/Phi-4-multimodal-instruct
1002 LLaVA-OneVision | llava-hf/llava-onevision-qwen2-7b-ov-hf
1003 SmolVLM | HuggingFaceTB/SmolVLM2-2.2B-Instruct
1004 Pixtral | mistral-community/pixtral-12b
1005

1006
1007
1008
1009
1010
1011
1012
1013
1014
1015
1016
1017
1018
1019
1020
1021
1022
1023
1024
1025

1026 **C HYPERPARAMETERS**
10271028 Table 3: LAPO-ResNet hyperparameters. Names are exactly follow the configuration files used in
1029 code.
1030

1031

1032

Part	Parameter	Value
General	frame_stack	4
	probe_learning_rate	0.0003
	disable_distractors	True
	seed	0
	eval_seed	0
	eval_episodes	50
Latent action learning	latent_action_dim	128
	idm_encoder_scale	5
	idm_encoder_num_res_blocks	1
	idm_encoder_channels	[16, 16, 32, 32, 128, 128, 256]
	fdm_encoder_scale	1
	fdm_encoder_num_res_blocks	1
	fdm_encoder_channels	[16, 16, 32, 32, 128, 128, 256]
	num_epochs	10
	batch_size	64
	learning_rate	0.0001
Latent behavior cloning	weight_decay	0.0
	warmup_epochs	0
	encoder_scale	5
	encoder_num_res_blocks	1
	encoder_channels	[16, 16, 32, 32, 128, 128, 256]
	total_updates	100000
	batch_size	64
Latent actions decoding	learning_rate	0.001
	hidden_dim	128
	num_labeled_trajectories	[16, 8, 2, 4]

1065

1066

1067

1068

1069

1070

1071

1072

1073

1074

1075

1076

1077

1078

1079

Table 4: LAPO-Trans hyperparameters. Names exactly follow the configuration files used in code.

Part	Parameter	Value
General	frame_stack	4
	probe_learning_rate	0.0003
	disable_distractors	True
	seed	0
	eval_seed	0
	eval_episodes	50
Latent action learning	latent_action_dim	128
	patch_size	32
	fdm_use_cross_attn	False
	idm_hidden_dim	896
	idm_num_layers	4
	idm_num_heads	16
	fdm_hidden_dim	256
	fdm_num_layers	4
	fdm_num_heads	8
	normalize_qk	False
	pre_norm	True
	num_epochs	10
	batch_size	64
	learning_rate	0.0001
	weight_decay	0.0
	warmup_epochs	1
	grad_norm	-
Latent behavior cloning	num_epochs	10
	batch_size	64
	learning_rate	0.0001
	weight_decay	0.0
	warmup_epochs	0
	encoder_scale	5
	encoder_num_res_blocks	1
Latent actions decoding	encoder_channels	[16, 16, 32, 32, 128, 128, 256]
	total_updates	100000
	batch_size	64
	learning_rate	0.001
	hidden_dim	128
	num_labeled_trajectories	[16, 8, 2, 4]

1134
1135
1136
1137
1138
1139
1140

1141 Table 5: LAPO+VLM hyperparameters. Names exactly follow the configuration files used in code.

1142
1143

Part	Parameter	Value
General	frame_stack	4
	probe_learning_rate	0.0003
	disable_distractors	True
	seed	0
	eval_seed	0
	eval_episodes	50
VLM (example)	type	molmo
	prompt	Point to the robotic arm gripper.
	layer	27
	target	output
	reduce_strategy	mean
Latent action learning	latent_action_dim	128
	idm_encoder_scale	5
	idm_encoder_num_res_blocks	1
	idm_encoder_channels	[16, 16, 32, 32, 128, 128, 256]
	fdm_hidden_dim	1024
	fdm_num_layers	4
	fdm_expand	4
	num_epochs	200
	batch_size	64
	learning_rate	0.0001
	weight_decay	0.0
	warmup_epochs	1
	grad_norm	-
Latent behavior cloning	num_epochs	10
	batch_size	64
	learning_rate	0.0001
	weight_decay	0.0
	warmup_epochs	0
	encoder_scale	5
	encoder_num_res_blocks	1
	encoder_channels	[16, 16, 32, 32, 128, 128, 256]
Latent actions decoding	total_updates	100000
	batch_size	64
	learning_rate	0.001
	hidden_dim	128
	num_labeled_trajectories	[16, 8, 2, 4]

1181
1182
1183
1184
1185
1186
1187